ИНСТИТУТ ЯДЕРНОЙ ФИЗИКИ СО АН СССР

17

V.V.Anashin, I.B.Vasserman, A.M.Vlasov,
P.V.Vorobjev, P.M.Ivanov, P.A.Klimin,
I.A.Koop, E.A.Perevedentsev,
A.N.Skrinsky and Yu.M.Shatunov

THE 75 KG SUPERCONDUCTING WIGGLER MAGNET FOR THE ELECTRON-POSITRON STORAGE RING VEPP-2M

PREPRINT 84-123

НОВОСИБИРСК

The superconducting wiggler magnet with the maximum field of 75 kG will be installed on the electron-positron storage ring VEPP-2M [1] for significant enhancement of the colliding beams luminosity in the energy range from 2 x 200 MeV to 2 x 700 MeV. In addition to the high energy physics program purposes the wiggler will be operated as a synchrotron radiation source.

The wiggler parameters were optimized to attain the luminosity of about $2 \cdot 10^{31}\ cm^{-2} sec^{-1}$ in the energy range of φ-meson (2 x 510 MeV) without serious changes in the storage ring magnetic structure and design. The accepted version consists of three central 75 kG dipoles and two side 45 kG dipoles. The wiggler is placed in one of the experimental straight sections which enables the exit of the synchrotron radiation from both the electron and positron beams to both existing SR laboratories.

The limitation on the wiggler length of 60 cm and the side dipoles field of 45 kG are put by the possibilities to compensate the perturbations from the wiggler in the VEPP-2M magnetic structure and by the β_z growth on either side of the straight centre (β_{zo} = 6.4 cm) to the adjacent quadrupoles (β_z^{max} = 550 cm). The beam injection conditions the vertical beam stay clear size of the inner chamber of the wiggler of 15 mm.

VEPP-2M luminosity with the wiggler

The electron-positron colliding beams luminosity is given for $\varepsilon_x \gg \varepsilon_z$ by the well-known equation [2,3] :

$$\mathcal{L} = \frac{\pi \cdot \gamma^2 \cdot \xi_x \cdot \xi_z \cdot (1 + \sigma_{zo}/\sigma_{xo})^2 \cdot f_o \cdot \varepsilon_x}{r_e^2 \cdot \beta_{zo}}$$

where ξ_x and ξ_z are the space charge parameters for „x" and „z" motion where of the maximum is limited by the beam-beam effects; σ_{xo} and σ_{zo} are the beam r.m.s. sizes at the collision point; ε_x is the horizontal beam emittance; f_o is the revolution frequency; β_{zo} is the β-function value at the collision point; r_e is the electron classical radius and γ is the relativistic factor.

It is evident from the equation that the maximum luminosity is proportional to the horizontal beam emittance. The attempts to benefit from this dependence for the higher luminosities have been made on VEPP-2M by means of blowing the horizontal betatron or the synchrotron oscillations with the noise excitation. However the controlled colliding beams sizes and horizontal emittances growth seemed to be precluded by the coherent component in the oscillation spectrum. Apparently employing the quantum fluctuations of the synchrotron radiation gives the perfect means for the controlled build-up of the transverse emittance in the electron-positron storage rings.

Incorporating the wiggler into the storage ring magnetic structure will result in the luminosity enhancement due to enlarged horizontal emittances of the beams that the higher values of the parameters ξ_x and ξ_z will be obtained due to the stronger radiation damping and the corresponding reduction of the beam-beam effects.

There is also the way to higher luminosities based on reduction of β-function at the collision point. The storage ring VEPP-2M is operated with "mini-β_{z0}" of about 2.7 cm at the energy of 510 MeV since the end of 1982 and thus gams a factor of 1.7 in luminosity as compared with the four-fold mirror-symmetric lattice (β_{z0} = 6.4 cm). The further reduction of β_{z0} does not result in luminosity raising because the β-function at the collision becomes less than the bunch length.

The horizontal beam emittance ε_{xw} with the account of the wiggler field H_w can be written in the following form:

$$\varepsilon_{xw} = \varepsilon_x \cdot \frac{J_x}{J_{xw}} \cdot \frac{1 + \int |H_w(s)|^3 \cdot I_w(s) \cdot ds / \int |H_M|^3 \cdot I_M(s) \cdot ds}{1 + \int |H_w(s)|^2 \cdot ds / \int |H_M|^2 \cdot ds},$$

where ε_x is the horizontal emittance with the wiggler field off; $J_x = G_x/G_z$ is the ratio of the damping rates for the horizontal and vertical betatron oscillations; $I_w(s), I_M(s) = \gamma_x \eta_x^2 + 2\alpha_x \eta_x \eta_x' + \beta_x \eta_x'^2$ are the Courant-Snyder "invariants" for the horizontal dispersion function $\eta_x(s)$; $\gamma_x(s)$, $\alpha_x(s)$, $\beta_x(s)$ are the Twiss parameters; H_M is the field value in the storage ring bending magnets; the subscript "w" relates to the magnetic structure with the wiggler field on.

For the case where the contribution of the wiggler field into the excitation and damping the horizontal betatron oscil-

lation amplitudes dominates over that of the bending magnets, the horizontal emittance is approximately written as follows:

$$\varepsilon_{xw} \approx \varepsilon_x \cdot \frac{J_x}{J_{xw}} \cdot \frac{|H_w|}{|H_M|} \cdot \frac{\langle I_w \rangle}{\langle I_M \rangle}$$

it is practically independent of the wiggler length. Here $\langle I_M \rangle$ is the average of $I_M(s)$ over the length of the bending magnets of the storage ring. Note that the horizontal emmittance control can be effected both by variation of the field value H_w and by variation of $I_w(s)$ averaged over the wiggler length $\langle I_w \rangle$ at $H_{w\,max}$ kept constant.

At the energy of 510 MeV and H_w=75 kG we obtain $\varepsilon_{xw}/\varepsilon_x = 5$, ($\langle I_w \rangle$=66.4 cm, $\langle I_M \rangle$=19.7 cm, J_x=0.616, J_{xw}=0.864). For the wiggler field off we have I_w = 35.7 cm over the the straight section. The further increase of ε_{xw} within the existing magnetic aperture is limited by the experimetally observed reduction of $(\xi_x)_{max}$ on VEPP-2M for the ratio of aperture to the total horizontal beam size $A/\sigma_{x\,tot} \sim 8$ due to the beam-beam interaction.

The higher threshold values of $(\xi_x)_{max}$ and $(\xi_z)_{max}$ will additionally gain a factor of 1.7 in luminosity, assuming $(\xi_x)_{max}$ and $(\xi_z)_{max} \sim \tau_{x,z}^{-1/3}$, $\tau_{x,z}$ standing for the damping time [3]. Thus the luminosity will increase by a factor of 8.5 over the energy range $250 < E \leqslant 510$ MeV.

For the energies lower than 250 MeV the beam emittances are determined by the multiple intrabeam scattering (MIS) [3] and the gain in luminosity comes from the increase in the radiation damping rates only. In figs 1 and 2 the computed dependence of the luminosity and the proposed variation of the wiggler field on the energy are shown. The lower curves correspond to the limited positron production rate of $\approx 10^7 e^+$/sec on VEPP-2M at present. After implementation of the new booster storage ring BEP [4] which will give the positron production rate of $10^8 e^+$/sec, the luminosity on VEPP-2M will come to 7×10^{31} cm^{-2}sec^{-1} at 700 MeV. This value is the upper limit for the mean luminosity on VEPP-2M because the rate of the particle losses due to the single bremsstrahlung on the opposite beam $\dot{N}^+_\gamma$ will practically match the rate of the positron accumulation $\dot{N}^+$.

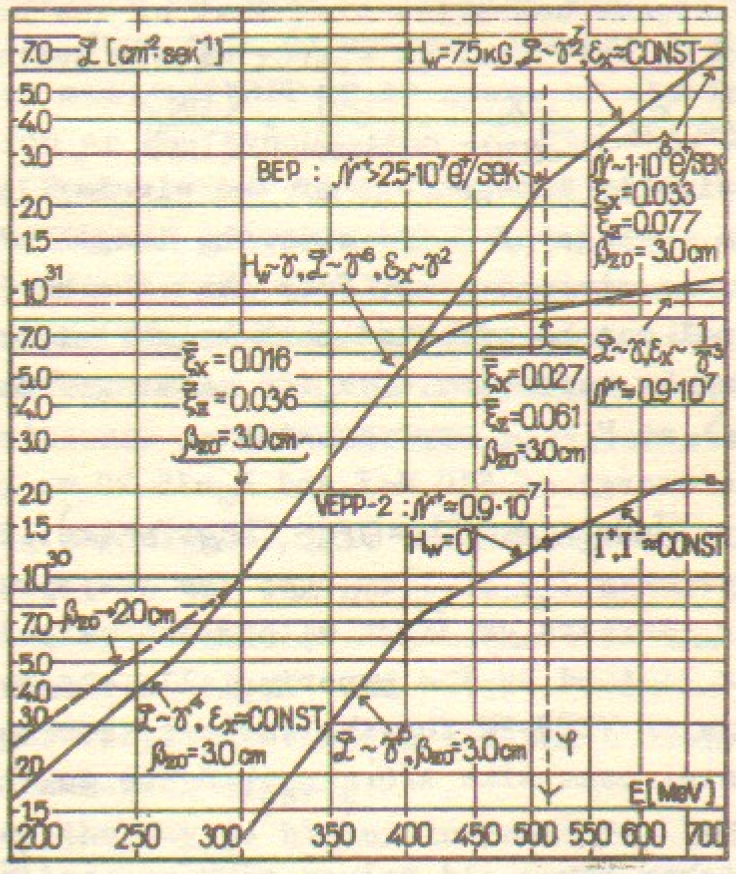

Fig.1

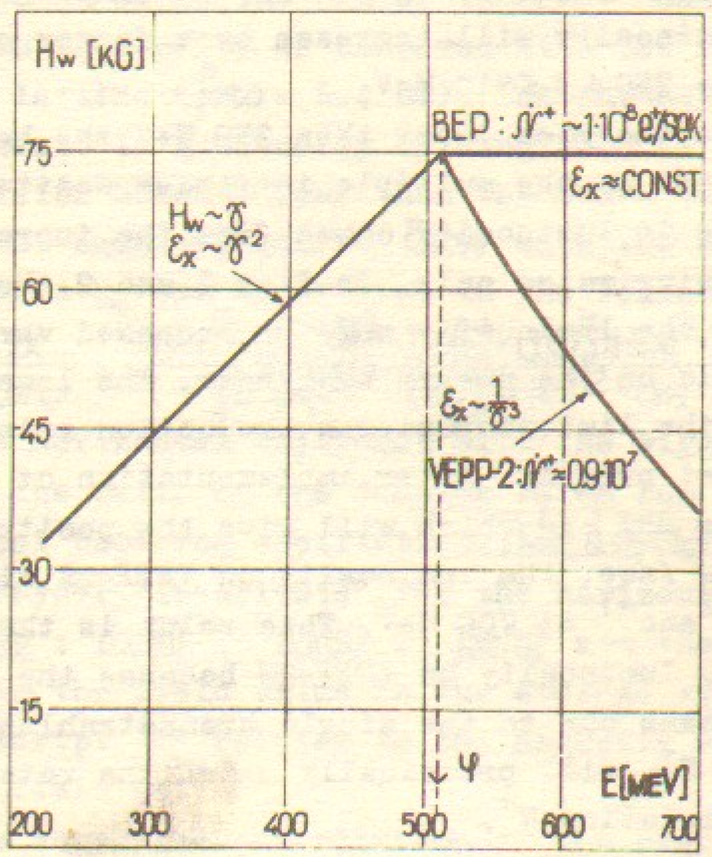

Fig.2

Table 1. Beam parameters with the wiggler field off and on

Energy E = 510 MeV, β_{z0} = 3.0 cm, emittance coupling ratio $\varkappa$=0.1		units	H_w= 0	H_w=75 kG
Horizontal emittance $\mathcal{E}_x$ x 10^5		cm.rad	1.08	5.0
R.m.s. beam sizes at the collision point	σ_{z0}	mm	0.007	0.014
	σ_{x0}		0.27	0.059
Radiation damping times	τ_z	msec	12.41	6.85
	τ_x		20.00	7.92
	τ_s		5.17	3.20
Beam lifetime due to MIS Current 100 mA, $(\Delta E/E)_{max}$=0.5%		sec	178	2000
Radiation energy loss per turn		keV	5.0	9.07
R.m.s. beam energy spread $\sigma(\Delta E/E)$ x 10^3			0.36	0.60
Beam currents limited by the beam-beam interaction		mA	18	100

Focusing in the wiggler field

The particle beam passing through the alternating (approximately sinusoidal) wiggler field is subject to the vertical edge focusing. For the horizontal motion the edge defocusing is totally compensated by the sector focusing in the horizontal bends. At the energy of 510 MeV and the wiggler field H_w= 75 kG the vertical tune shift comes to $\Delta\nu_z\sim 1$ and the vertical motion becomes unstable when crossing the integer stopband ν_z=4. To avoid this the compensation of the wiggler focusing is envisaged with the gradient corrections in the main quadrupoles of the storage ring.

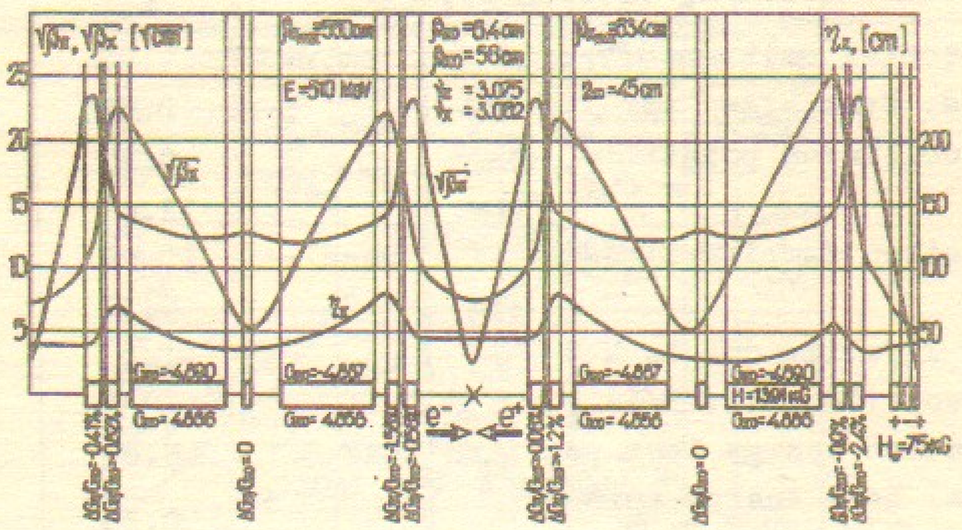

Fig.3

Fig.3 shows the lattice of the storage ring VEPP-2M which is mirror-symmetric with respect to the wiggler centre. The four-fold mirror symmetry of the initial lattice though broken by the wiggler insertion is restored by the corrections fairly good as one can see from the graphs of βz , βx and ηx . Here $\Delta G/G_0 \times 100\%$ are the needed values of the gradient corrections in the quadrupole lenses.

This lattice is wanted for the beam injection. To control $\beta z0$ at the collision point another lattice is envisaged with the double mirror symmtry (see fig.4). Switching the lattice to the four-fold symmetry for each injection takes about 4 seconds.

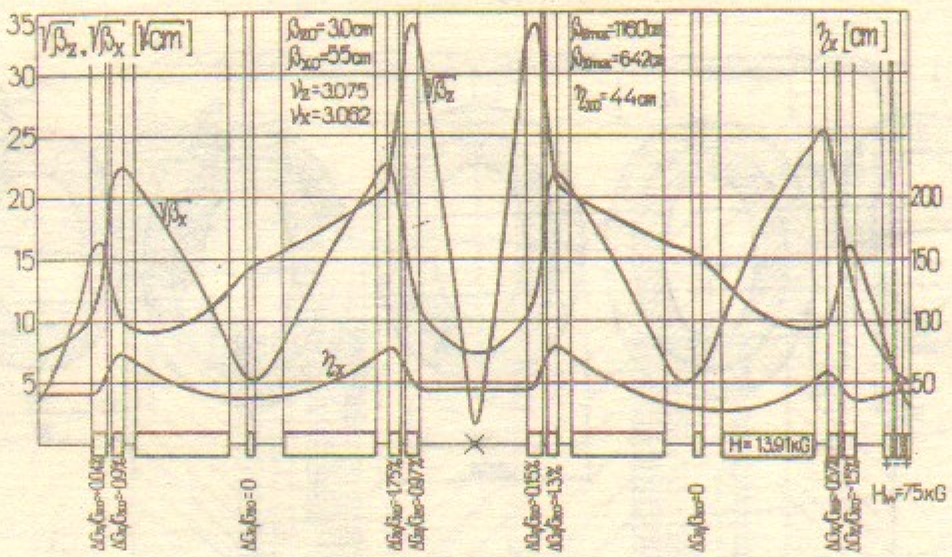

Fig.4

The field decomposition $(H_z)'_x$ having sextupole and decapole components and the design orbit traversing the alternating wiggler field with the variable horizontal displacement $x \neq 0$, the additional focusing arises and also the betatron tune dependence on the amplitude.

To cancel the quadrupole component of the field integral $\int \frac{\partial Hz(z,x,s)}{\partial x} \cdot ds$ along the orbit the dipoles are shifted in the horizontal plane so that in each dipole the orbit passed with the displacement $x > 0$ (with respect to the dipole's centre line) in one part of its length and with $x < 0$ in another one. Such shifts also result in the suppression of the cubic non-linearity over each dipole's length. The values $\frac{\partial \nu z}{\partial a_z^2}$ and $\frac{\partial \nu x}{\partial a_x^2}$ are of the order of $10^{-4} cm^{-2}$ and do not influence the beam dynamics within the storage ring aperture. The horizontal shifts of the neighbouring dipoles for the specific configuration of the VEPP-2M wiggler comes to $2x\langle X\rangle$=9.4 mm(fig.5). The computed three-dimensional field patterns were used as obtained from "MAG-3D" computer code [5] which accounts for saturation in the iron cores and yokes.

The initial optimization was based on simplified calculation of elliptic dipoles with iron cores assumed totally saturated and uniformly magnetized.

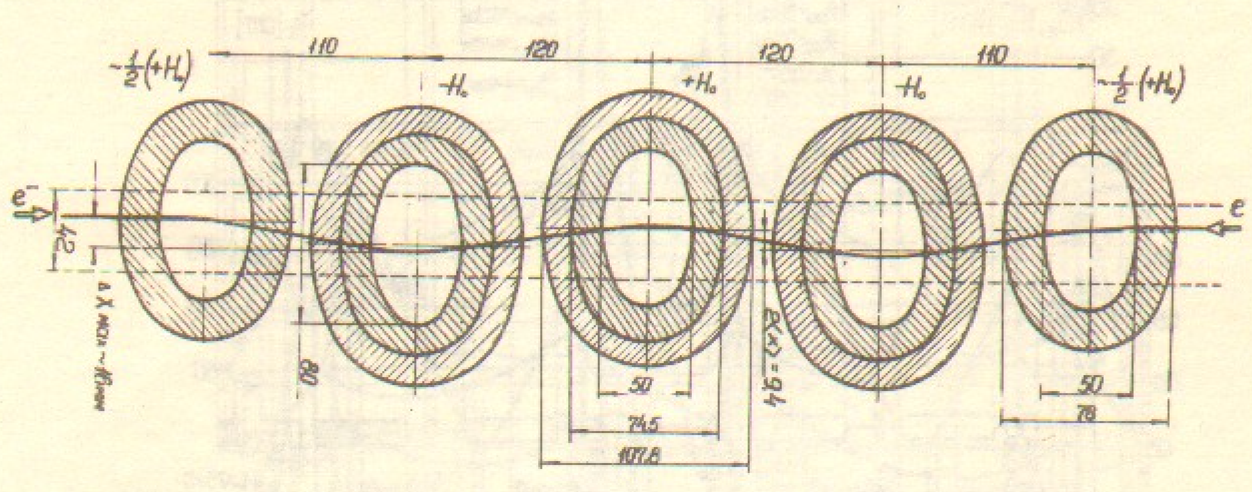

Fig.5

<u>Features of the VEPP-2M wiggler design</u>

The wiggler design is shown in figs. 5-7, its parameters are listed in tables 2 and 3. The lower and the upper poles of the dipoles are housed in two separated helium vessels which are joined with an accuracy of $\pm 50\mu m$ to form the block of superconducting magnets. The inner vacuum chamber kept under nitrogene temperature is placed in the middle of the SC magnet block with the spacing of 1.5 mm. The replacement and assembly of the SC magnets can be performed with the storage ring vacuum retained. The doubled helium vessel with the dipoles is fixed to the nitrogene tank via the leaf supports, and the tank is hang on the support arms mounted on the outer shell base. The support type employed provides for the stable position of the SC magnet block with respect to the median plane in cooling and against the magnetic forces. The construction is housed in the removable vacuum-tight housing serving also as a stray flux yoke.

For the independent supply of the central and side dipoles three feedthroughs are used. The liquid helium is supplied

by the separate dewar tank of 145 little capacity similarly to [6].

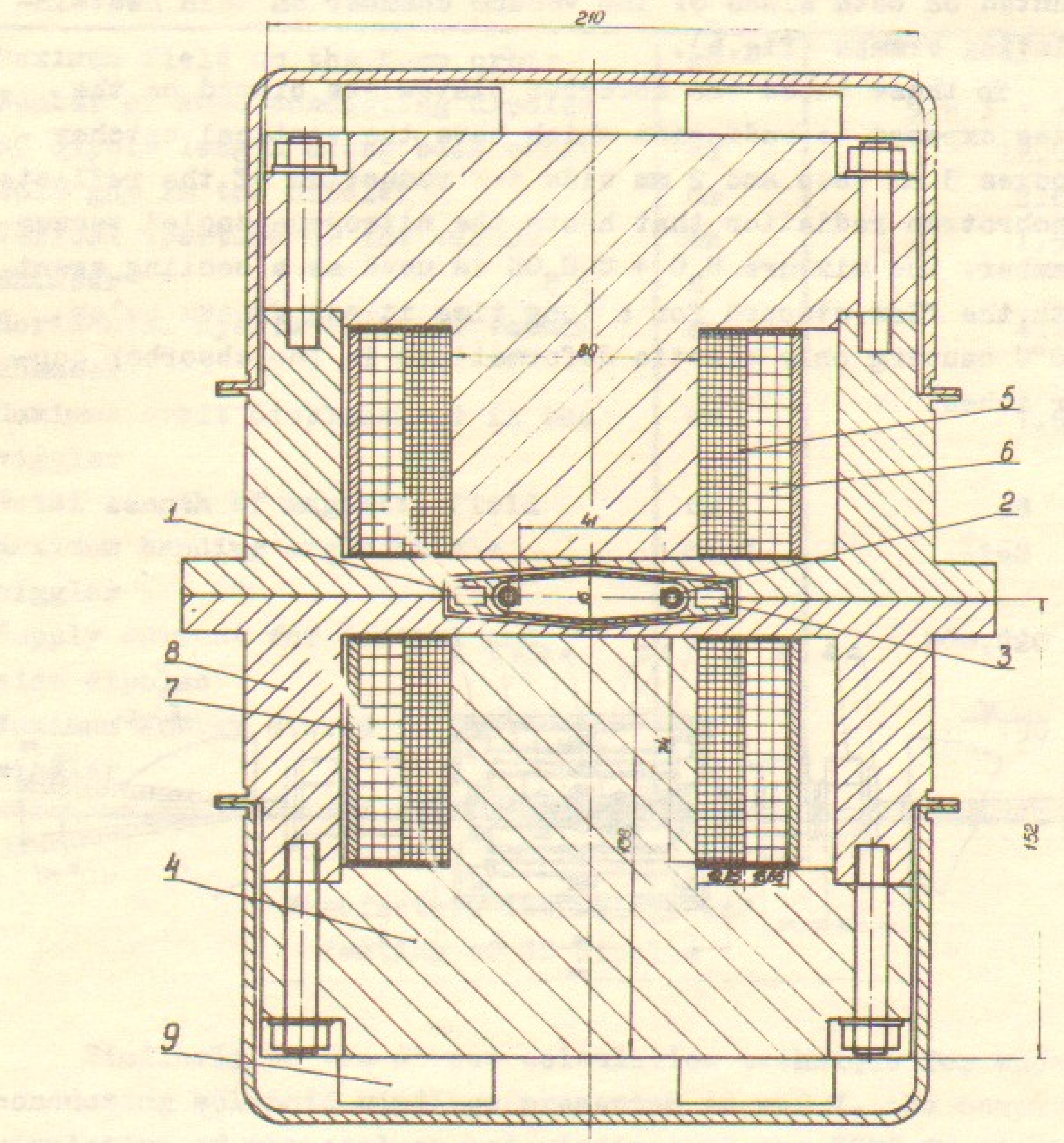

Fig.6. Vertical cross-section of the superconducting wiggler magnet for VEPP-2M.

1 - vacuum chamber, 2 - cooled absorber for synchrotron radiation, 3 - liquid introgene duct, 4 - iron core, 5 - inner winding section, 6 - outer winding section, 7 - wire binding, 8 - stainless steel helium vessel, 9 - shunt resistors.

The half of the synchrotron radiation power generated by the wiggler does not escape the inner vacuum chamber thus urging the special cooled absorbers for synchrotrnn radiation to be developed. The absorbers are made of copper tube with inner diametres of 4mm and wall thickness of 1mm, they are mounted on both sides of the vacuum chamber on thin heat-insulating cramps (fig.6).

To these tubes the absorber plates are brazed on the sides exposed to radiation which have the vertical catcher grooves 3 mm deep and 2 mm wide for reduction of the reflected synchrotron radiation that heats the nitrogene-cooled vacuum chamber. The mixture $H_2O + C_2H_5OH$ is used as a cooling agent. With the flow stopped for a long time it can freeze below -60°C causing only elastic deformations in the absorber copper tubes.

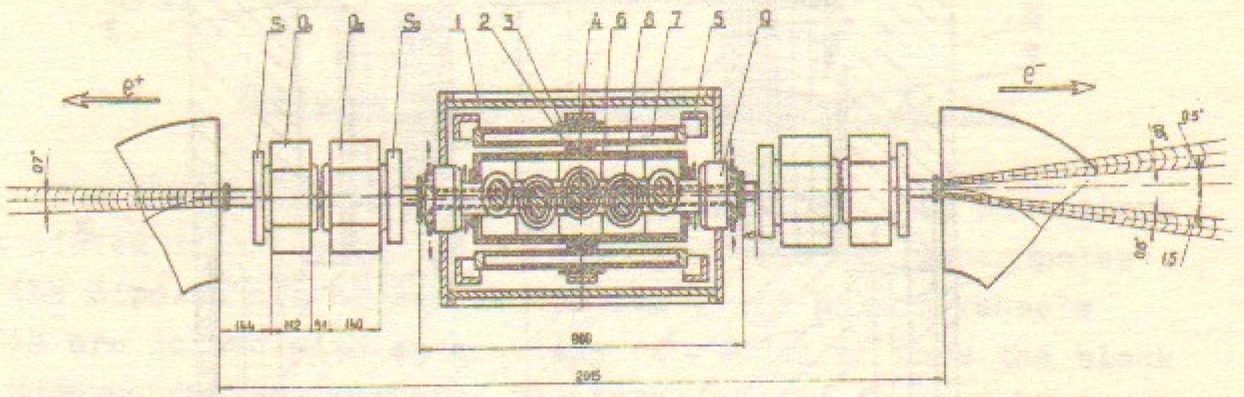

Fig.7. VEPP-2M straight section with the superconducting wiggler magnet. Q_x and Q_z are quadrupole lenses, S_x and S_z are sextupole correctors, 1 - stray flux yoke and housing, 2 and 3 - leaf supports, 4 and 5 - arm supports, 6 - helium vessel, 7 - nitrogene vessel, 8 - inner vacuum chamber, 9 - assembly of heat insulation and absorbers feedthrough. Synchrotron radiation ports and lines are shown schematically.

Table 2. Design parameters of the superconducting wiggler magnet on VEPP - 2M

Maximum field on the beam orbit	kG	75
Number of superconducting dipoles		5 = 3 + 2
SC dipole length along beam orbit	cm	12.0
Pole gap in the dipoles	cm	2.65
Verical aperture of the vacuum chamber	cm	1.50
Horizontal aperture of the vacuum chamber	cm	4.2
Maximum orbit displacement in the wiggler	cm	1.6
Total length of magnetic field	cm	58
Maximum bending angle in the wiggler	mrad	±168
Supply current for central and side dipoles	A	200,220
Maximum energy stored in the wiggler	kJ	150

Manufacture technology and testing of SC dipoles

Similarly to the stress calculation technique for superconducting solenoid windings presented in ref.7, the computer simulation of the oval shaped windings of the VEPP-2M wiggler dipoles was carried out for the stages of winding the superconducting wire over the iron core, applying the bind, cooling down liquid helium temperature and powering the current. The analysis was made of the tangent stress in the wire, compression of each layer of winding and radial strain of the layers. The main purpose of the simulation was to reveal beforehand the possible reasons of superconductor degradation so as to avoid them before winding manufacture. Optimizing the dipole winding technology we conjectured the mechanical origins of degradation.

The most serious were the apprehensions of the following faults:

- local concentration of tangent stresses along the azimuthal direction in the winding;
- stepwise change in the wire strain in the neighbouring layers of windings and between the sections;
- rise of large strains from thermomechanical forces during cooling.

Pre-tensioning of the wire during winding it up was found out to be insufficient by itself to prevent degrading which results from mobility of turns when the field is raised up to 75-80 kG. Therefore epoxy monolyth cementation of the winding is necessary.

The oval shaped core having two different curvature radii R_{max}=6.25cm and R_{min}=2.0cm, the acceptable uniformity of tangent stress in radial and azimuthal directions put the upper limit upon the winding thickness of 3 cm.

The difference in the integrated thermal contraction coefficient of the winding and the core (made of armco iron) being $\approx 1\times10^{-3}$ in the range from the room temperature down to that of liquid helium, an elastic spacer is necessary between the core and the innermost layer of the winding. The spacer was made of lavsan film 20 m thick wound in 10 layers. The lavsan film compensates the unwanted breaking action of the core in radial direction and provides for thermomecanical stress relief in vertical direction.

The adhesive for impregnation is the hot-hardening epoxy compound composed of epoxy resin "ED-16"(100 parts by weight) + triethanolamine (10 p.w.) + Al_2O_3(70 p.w.). The polymerization is performed in two stages: 10 hours at 80°C then 10 hours at 120°C. Such a condition for polymerization is aimed at the minimum shrinkaze of the compound and its maximum resistance against thermal shocks.

The layer-to-layer insulation is made of three layers of glass veil 20 m thick. The winding impregnation was continiously done by pulling the wire through the epoxy compound container. The needed thickness of the adhered compound layer was controlled by varying the outlet diameter in the container spinneret. The core and the adhesive compound were thermally stabilized at 55°C.

The windings were wound by the superconducting wire made of Nb-Ti alloy NT-50 in copper matrix with enamel insulatuion. The wire tension in winding up was automatically controlled with an accuracy of ± 0.05kg(f) and for each layer the computed value was applied. Maximum tension was 7.7kg for the inner section and 4.0 kg for the outer one. The bind of stainless steel wire of 1.0 mm in diameter was wound in four layers with the tension of 23.5 kg.

Table 3 Parameters of the windings and the superconducting wire

	inner section	outer section	SC winding of side dipoles
Winding height (mm)	74	74	74
Winding thickness(mm)	12.25	16.65	14.20
Number of turns	785	2014	1216
Nb-Ti/Cu wire diameter (mm)	1.0	0.7	0.85
Space factor of the SC alloy	0.475	0.485	0.470
Number of SC filaments	54	54	60

During the period from late January to March 1984 12 superconducting poles were manufactured of which 8 were for the central dipoles and 4 for the side ones. For testing they were assembled by couples to form a dipole block with the pole gap of 26.5mm(see fig.6). The blocks were plunged in the helium cryostat and powered with current. After 30-35 cycles of quenching the field in the gaps of all the central dipoles was raised to $\approx$ 77kG. The further field rise was limited by appearance of the critical current of short sample at H_{max}=81kG in the inner section of the winding (namely, 98 per cent of I_c for short sample for the specified field at 4.2°K). Fig.8 shows the short sample characteristics for the two types of wire used and current dependencies for H_{max} in the inner and outer sections of the winding. In fig.9 one can see the progress and number of quenching cycles for one of the central dipoles.

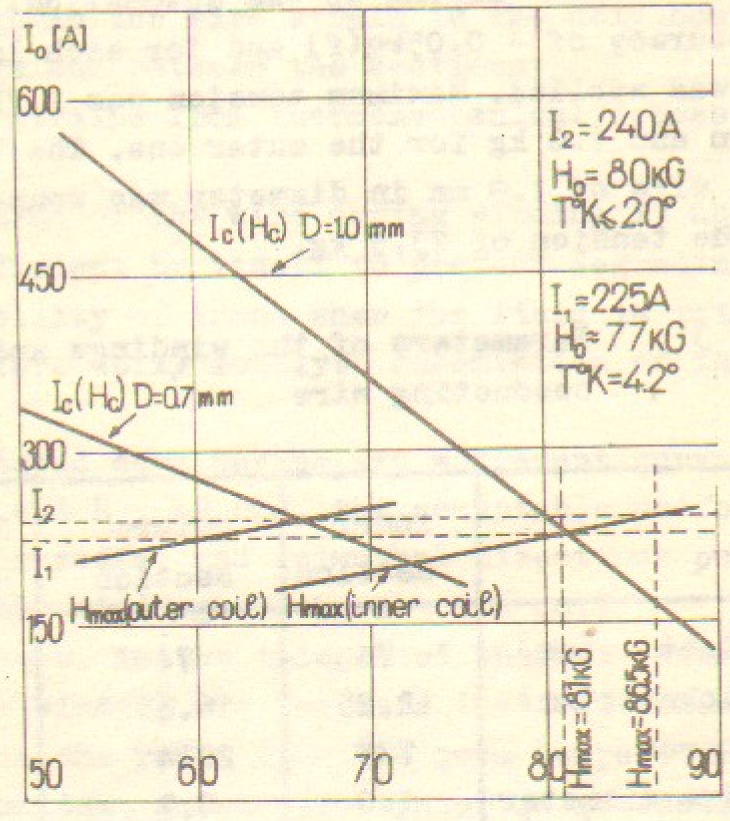

Fig.8

For the three central dipole blocks several additional quenching cycles were performed with pumping helium down to pressure ≈ 35 torr in the cryostat (corresponding to $\lesssim 2°K$). This resulted in raising the field up to 78-80kG in each of the dipoles. For field value of 80kG in the gap the field in the winding inner sections comes to 86.5kG at the current I_2 = 240A.

In the side dipoles the gap field reached $\approx$ 52.5kG after several quenching cycles which is also close to the upper limit.

During the tests the magnetic field was measured in the centre of the pole gap with the Hall probe at liquid helium temperature. In the wide range of the field from low values up to 80kG the Hall probe signal was linear with the accuracy within 0.1 per cent.

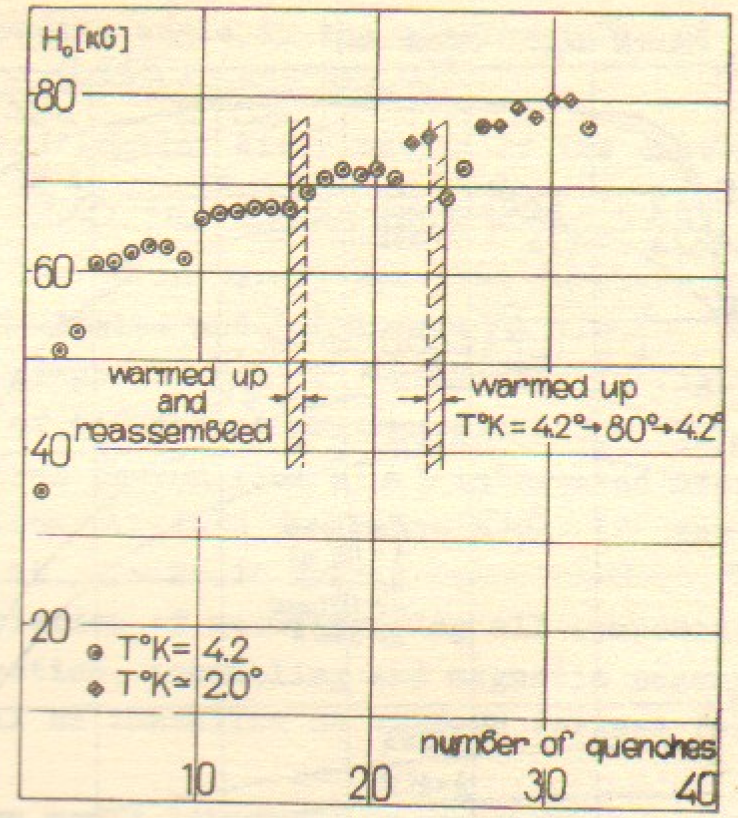

Fig.9

Characteristics of the synchrotron radiation from the VEPP-2M wiggler magnet

The detailed analysis of SR characteristics for the wiggler source can be found in ref.8. Here only a few SR characteristics are presented calculated by the formulae from ref.8 with the account of specific parameters of the VEPP-2M wiggler.

The total radiated power is given by the equation:

$$W[w]=2.691\cdot 10^{-3}\cdot E^2\cdot[GeV]\cdot H^2_{W max}[\kappa G]\cdot I[mA]$$

The radiation critical wavelength is

$$\lambda_{co}[A^o]=\frac{186.4}{E^2[GeV]\cdot H_{W max}[\kappa G]}$$

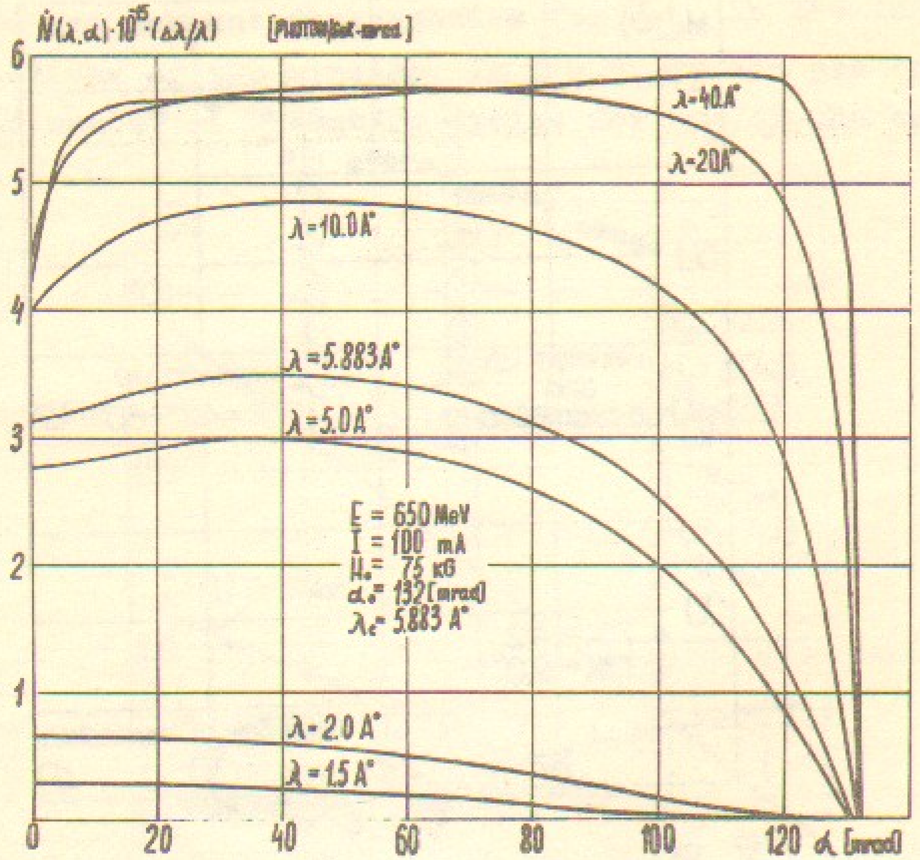

Fig.10

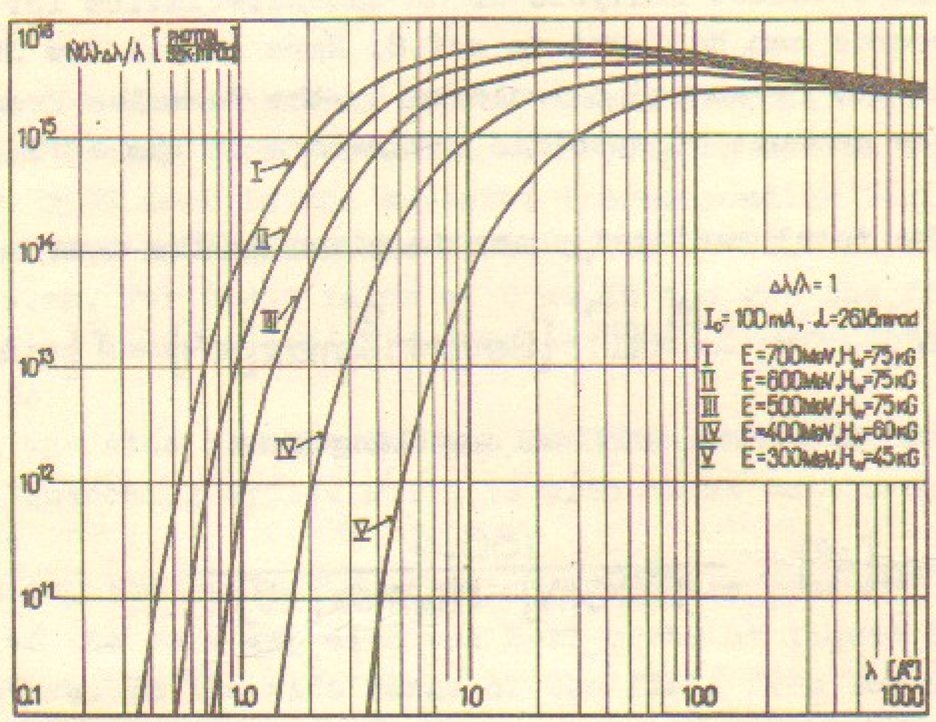

Fig.11

Maximum bending angle in the wiggler is

$$\alpha_o[mrad] = \frac{1.145 \cdot H_{w\,max}[kG]}{E[GeV]}$$

Spectral and angular distribution of the photon flux is

$$\dot{N}(\lambda,\alpha)\left[\frac{PHOTON}{sek \cdot mrad}\right] = 2.457 \cdot 10^{13} \cdot E[GeV] \cdot I[mA] \cdot \left[3\eta(y_\alpha) + \eta(\tilde{y}_\alpha)\right] \cdot \frac{\Delta\lambda}{\lambda},$$

where $\eta(y_\alpha)$ is the SC universal spectral function, $y_\alpha = \frac{\lambda_{co}}{\lambda}\sqrt{1-\left(\frac{\alpha}{\alpha_o}\right)^2}$ for the central dipoles and $\tilde{y}_\alpha = \frac{\lambda_{co}}{\lambda} \cdot 0.833 / \sqrt{\frac{\alpha}{\alpha_o}\left(1-\frac{\alpha}{\alpha_o}\right)}$ for the side ones. The graphs of $\dot{N}(\lambda,\alpha)$ are shown in fig.10 for the energy of 650 MeV at maximum field H_w = 75kG. Fig.11 shows the spectral photon flux $\dot{N}(\lambda)$ integrated over vertical angles for various λ into the range $\Delta\lambda/\lambda = 1$ per unit horizontal angle at α = 26.18 mrad.

After completion of manufacturing all components of the wiggler construction, assembling and magnetic measurements the wiggler will be installed on VEPP-2M (planed for September 1984).

The authors would like to express their acknowledgements to L.M.Barkov and G.N.Kulipanov for their interest in the work and useful discussions of the project, to M.A.Tiunov and V.F.Pindiurin for the possibility to use the computer programs calculating magnetic fields and SR spectra, to A.A. Mikhailichenko for his help in magnetic measurements and to the large group of VEPP-2M technicians who contributed to manufacturing and testing the superconducting magnets.

References

1. G.M.Tumaikin "Electron-positron storage ring with high luminosity VEPP-2M" Proc. Xth Int.Conf.on High Energy Particle Accelerators, Protvino, v.1, p.443, 1977.
2. I.B. Vasserman et al. "Status of the electron-positron storage ring VEPP-2M". Proc. 6th All-Union Conf. on Charged Particles Accelerators, Dubna, v.1, p,136, 1979.
3. I.B. Vasserman et al. "Status of the electron-posotron storage ring VEPP-2M". Proc. 7th All-Union Conf. on Charged Particles Accelerators, Dubna, v.1, p.242, 1981.

4. Internal Report. "Storage Ring BEP". INP preprint 83-98.
5. M.A.Tiunov, B.M.Fomel. "Computation of three-dimensional magnetic systeme with iron", INP preprint 83-150.
6. A.S.Artamonov et al. "First results of the work with a superconducting "shake" on VEPP-3 storage ring", NIM, 177 (1980), 239-246.
7. N.V.Krivolutskaya, A.I.Rusinov. "Computation of mechanical stress in composite material solenoid with the account of pre-tension of the turns" Lebedev Phys.Inst.Proc., v.121, p.14, 1980.
8. G.N.Kulipanov, A.N.Skrinsky "Application of synchrotron radiation: status and prospects", Sov. Phys. Uspekhi, v.122, p.309 (1977).

В.В.Анашин, И.Б.Вассерман, А.М.Власов,
П.В.Воробьев, П.М.Иванов, П.А.Климин,
И.А.Кооп, Е.А.Переведенцев, А.Н.Скринский,
Ю.М.Шатунов

СВЕРХПРОВОДЯЩАЯ "ЗМЕЙКА" С ПОЛЕМ 75 кГс ДЛЯ ЭЛЕКТРОН-ПОЗИТРОННОГО НАКОПИТЕЛЯ ВЭПП-2М

Препринт
№ 84-123

Работа поступила - 31 августа 1984 г.

Ответственный за выпуск - С.Г.Попов
Подписано к печати 13.09-84 г. МН 04530
Формат бумаги 60х90 1/16 Усл.1,4 печ.л., 1,1 учетно-изд.л.
Тираж 290 экз. Бесплатно. Заказ № 123.

Ротапринт ИЯФ СО АН СССР, г.Новосибирск, 90